



KTH Chemical Science
and Engineering

HNO₃-Induced Atmospheric Corrosion of Copper, Zinc and Carbon Steel

by

Farid Samie

Doctoral Thesis

This doctoral thesis will, with the permission of the Royal Institute of Technology in Stockholm, be presented and defended at a public disputation on Friday 8th of December 2006, 10.00 a.m. in room F3, Lindstedsvägen 26, Kungliga Tekniska Högskolan, Stockholm, Sweden.

Opponent:

Prof. Carlos Arroyave, Universidad de Antioquia, Facultad de Ingenieria, Medellin, Colombia

Supervisors:

Prof. Christofer Leygraf, Royal Institute of Technology, Stockholm, Sweden

Dr. Johan Tidblad, Corrosion and Metals Research Institute, Stockholm, Sweden

ISBN 91-7178-483-7

The figure on the cover shows an image of a laboratory exposed copper sample with the basic nitrate salt, gerhardtite, formed on its surface. The sample was exposed 7 days in an exposure chamber to $325 \mu\text{g m}^{-3}$ HNO_3 at 65 % RH, 25 °C and 0.03 cm s^{-1} air velocity.

Copyright © 2006 by Farid Samie.

All rights reserved. No parts of this thesis may be reproduced without permission from the author.

Author mobile: +46(0)704076788

Printed by: Universitetsservice US-AB, Stockholm 2006

ISBN 91-7178-483-7

Farid Samie, 2006

“HNO₃-Induced Atmospheric Corrosion of Copper, Zinc and Carbon Steel.”

Royal Institute of Technology (KTH) and
Corrosion and Metals Research Institute (KIMAB)

Abstract

The role of nitric acid (HNO₃) on the atmospheric corrosion of metals has so far received little or no attention. However, the last decades of decreasing sulphur dioxide (SO₂) levels and unchanged HNO₃ levels in many industrialized countries have resulted in an increased interest in possible HNO₃-induced atmospheric corrosion effects. In this study a new method was developed for studying the corrosion effects of HNO₃ on metals at well-defined laboratory exposure conditions. The method has enabled studies to be performed on the influence of individual exposure parameters, namely HNO₃-concentration, air velocity, temperature and relative humidity, as well as comparisons with newly generated field exposure data.

The corrosion rate and deposition rate of HNO₃ on copper was shown to follow a linear increase with HNO₃ concentration. The deposition velocity (V_d) of HNO₃ increased up to an air velocity of 11.8 cm s⁻¹. Only at a higher air velocity (35.4 cm s⁻¹) the V_d on copper was lower than the V_d on an ideal absorbent, implying the V_d of HNO₃ at lower air velocities to be mass-transport limited.

Within the investigated temperature range of 15 to 35 °C only a minor decrease in the HNO₃-induced copper corrosion rate could be observed. The effect of relative humidity (RH) was more evident. Already at 20 % RH a significant corrosion rate could be measured and at 65 % RH the V_d of HNO₃ on copper, zinc and carbon steel reached maximum and nearly ideal absorption conditions.

During identical exposure conditions in HNO₃-containing atmosphere, the corrosion rate of carbon steel was nearly three times higher than that of copper and zinc. The HNO₃-induced corrosion effect of copper, zinc and steel turned out to be significantly higher than that induced by SO₂ alone or in combination with either NO₂ or O₃. This is mainly attributed to the much higher water solubility and reactivity of HNO₃ compared to SO₂, NO₂ and O₃. Relative to SO₂, zinc exhibits the highest sensitivity to HNO₃, followed by copper, and carbon steel with the lowest sensitivity.

Extrapolation of laboratory data to an assumed average outdoor wind velocity of 3.6 m s⁻¹ enabled a good comparison with field data. Despite the fact that ambient SO₂ levels are still much higher than HNO₃ levels, the results show that HNO₃ plays a significant role for the atmospheric corrosion of copper and zinc, but not for carbon steel. The results generated within this doctoral study emphasize the importance of further research on the influence of HNO₃ on degradation of other materials, e.g. stone and glass, as well as of other metals.

Keywords: Nitric acid; Deposition velocity; Mass transport; Air velocity; Relative humidity; Temperature; Gerhardtite; FT-IR; Ion Chromatography; XRD

Author mobile: +46-(0)704076788

Preface

The experimental work presented in this thesis was performed at the Corrosion and Metals Research Institute (KIMAB), Stockholm, Sweden. I have had a central part in all the development of the exposure method, planning and analyses of the results presented in the thesis. In all papers I have been responsible for preparing a first version of the manuscripts. The contributions of the co-authors are summarized here:

Dr. Johan Tidblad - the daily supervisor who actively participated in discussions during the entire doctoral work and in proofreading of all papers.

Prof. Christofer Leygraf – the main supervisor who actively took part in discussions, supervising and proofreading of all papers.

Dr. Vladimir Kucera - general guidance and proofreading of paper I, IV and V.

List of Publications

The following papers are presented in this thesis, which in the text will be referred to by their roman numerals:

- I. F. Samie, J. Tidblad, V. Kucera, C. Leygraf,
Atmospheric corrosion effects of HNO₃ - method development and results on laboratory exposed copper,
Atmospheric Environment 39, 7362-7373 (2005)

- II. F. Samie, J. Tidblad, V. Kucera, C. Leygraf,
Atmospheric corrosion effects of HNO₃ - Influence of concentration and air velocity on laboratory exposed copper,
Atmospheric Environment 40, 3631-3639 (2006)

- III. F. Samie, J. Tidblad, V. Kucera, C. Leygraf,
Atmospheric corrosion effects of HNO₃ - Influence of temperature and relative humidity on laboratory exposed copper,
Atmospheric Environment, accepted for publication (2006)

- IV. F. Samie, J. Tidblad, V. Kucera, C. Leygraf,
Atmospheric corrosion effects of HNO₃ - comparison of laboratory-exposed copper, zinc and carbon steel,
Atmospheric Environment, submitted (2006)

- V. F. Samie, J. Tidblad, V. Kucera, C. Leygraf,
Atmospheric corrosion effects of HNO₃ - a comparison of laboratory and field exposed copper, zinc and carbon steel,
Journal of the Electrochemical Society, submitted (2006)

The following papers have resulted from work that is not presented in the thesis:

- VI. Z. Y. Chen, D. Persson, F. Samie, S. Zakipour, C. Leygraf,
The effect of carbon dioxide on sodium chloride induced atmospheric corrosion of copper,
Journal of the Electrochemical Society, 152 (12), B502 (2005)
- VII. J. Tidblad, V. Kucera, F. Samie, S.N. Das, C. Bhamornsut, L.C. Peng, K.L. So, Z. Dawei, L.T.H. Lien, H. Schollenberger, C.V. Lungu, D. Simbi,
Corrosion impacts of air pollution in developing countries,
Water, Air and Soil Pollution, accepted for publication (2006)

Contents

1. Introduction	1
1.1 Atmospheric corrosion – brief description	1
1.2 Trends of pollutants	3
1.3 Sources for HNO ₃ formation	3
1.4 Previous corrosion-related work with HNO ₃	4
1.5 Overview of MULTI-ASSESS and RAPIDC projects	5
1.5.1 MULTI-ASSESS	5
1.5.2 RAPIDC	5
1.6 Purpose of the study	6
2. Experimental	7
2.1 Experimental set-up.....	7
2.2 Difficulties, failures and modifications	9
2.3 HNO ₃ analysis	12
2.4 Preparation of samples	13
2.5 Estimation of HNO ₃ deposition.....	13
2.6 Gravimetical analysis	15
2.7 Corrosion product analysis	15
2.8 Field studies.....	15
3. Results and discussion	17
3.1 HNO ₃ effects on copper (Paper I, II and III)	18
3.1.1 Effects of concentration	18
3.1.2 Effects of air velocity	19
3.1.3 Effects of exposure time	21
3.1.4 Effects of temperature	22
3.1.5 Effects of relative humidity	22
3.2 Comparison of HNO ₃ effects on copper, zinc and carbon steel (Paper IV).....	24
3.3 Comparison of HNO ₃ effects relative to SO ₂ (Paper IV).....	26
3.4 Comparison of laboratory and field data (Paper V)	27
4. Concluding remarks	31
5. Future work	33
6. Acknowledgements	35
7. References	37

Papers I – V

1. Introduction

Ever since humanity explored the use of copper and iron several thousand years ago, it was obvious that the metals degrade with time. Systematic studies on atmospheric corrosion were initiated and conducted much later, in the early 20th century. Of great importance was W.H.J. Vernon, a scientist in England, who studied the influence of individual exposure parameters, such as sulphur dioxide (SO₂), temperature and relative humidity, on the corrosion of metals and alloys¹. The method for determination of the corrosion rate was based on gravimetric measurements. Today, after decades of research and development of methods and analytical tools the knowledge on atmospheric corrosion has reached new levels²⁻²⁶. However, there is a continuous need for further research, mainly due to rigorous restrictions for minimum service life time of materials and applications, more severe demands on, e.g., protection of cultural objects and on process industries, and also due to changing conditions in anthropogenic pollution.

1.1 Atmospheric corrosion – brief description

The atmospheric corrosion of metals is an electrochemical process, i.e. a process that involves charge transfer from one species to another. Of principal importance is the cathodic (electron donating) reaction, the anodic (electron accepting) reaction, and the adsorbed aqueous adlayer on the metal that permits electrochemical reactions to occur. An initially completely dry metal surface exposed in an ambient atmospheric environment will instantly absorb water and form the water adlayer. The thickness of this adlayer is mainly dependent on the relative humidity of the surrounding environment and can range from a few monolayers of water, invisible to the eye, to clearly visible water layers. As soon as an acidic pollutant dissolves in this adlayer its conductivity will increase and the electrolyte formed acts as a conducting medium for transport of charge, whereby the metal may corrode more rapidly. In atmospheric corrosion the anodic reaction is written as:



which is balanced by a cathodic reaction, usually oxygen reduction reaction:



The effect of a pollutant on the atmospheric corrosion of metals is dependent on several important properties of the pollutant, e.g. its water solubility, chemical reactivity and acidity. As an example, the relatively low water solubility of nitrogen dioxide (NO₂) in comparison to nitric acid (HNO₃) or sulphur dioxide (SO₂) leads to low NO₂ dissolution in the adlayer and, hence, less aggressive electrolyte (see Table 1). Another important factor for ranking the sensitivity of a metal to a specific gaseous pollutant is the deposition velocity, defined as the ratio of the rate of deposition of the gas towards the metal surface and its concentration in the atmosphere. Table 1 displays the solubility, in terms of Henry's laws constant, and the deposition velocity for a number of important gaseous corrosion stimulators. From the table it is evident that HNO₃ exhibits both high solubility and high deposition velocity relative to the other pollutants shown.

Table 1

Solubility and deposition velocity for atmospheric pollutants. Data from Ref. 27.

Pollutant	H [*] (mol L ⁻¹ atm ⁻¹)	Deposition velocity [†] (cm s ⁻¹)	
		Outdoor	Indoor
H ₂ S	0.10	0.38	0.03
SO ₂	1.2	0.01-1.2	0.05
NO ₂	0.007	0.02-0.8	0.006
O ₃	0.012	0.05-1	0.036
HNO ₃	2.1 x 10 ⁵	0.1-30	0.07

* Henry's law constant

† The author has compiled and summarized data from other investigations.

The protective or passivating ability of a corrosion product layer formed on the metal surface depends on physical and chemical properties of the layer, as well as its distribution, morphology and adhering properties. The nature of corrosion products is important also for other reasons, and can be used to link the degradation of exposed materials to the pollutants responsible for the degradation.

1.2 Trends of pollutants

The control of anthropogenic sources is of great concern for legislators and environmental organizations, since many pollutants possess harmful effects on human health and on the environment, e.g. by increasing the corrosion rate of materials. The latter is of major importance from an economical, safety, environmental and esthetical point of view. Corroded construction materials often lead to reduced service life and economic loss, whereas degradation of historical monuments and objects may in addition cause considerable esthetical changes and indirect economic loss.

Decades of research on the corrosion effects of sulphur dioxide (SO₂) and international policy actions have led to significant reduction in concentration of this gas in most industrialized countries. Due to the reduction of SO₂ concentration, the relative effects of other pollutants, e.g. nitric acid (HNO₃), ozone (O₃) and nitrogen dioxide (NO₂) on the corrosion of materials have increased. Also, investigations have reported elevated levels of nitrogen compounds, O₃ and particulates²⁸, which has created a new multi-pollutant situation. There are few published data on ambient HNO₃ levels and these ranges from 1 to 20 µg m⁻³ in urban atmospheres²⁹⁻³³. In a recent study Ferm et al. (2005) reported unchanged levels of HNO₃ within the last decade at a Swedish background station³⁴. Other studies have suggested increased concentrations of HNO₃ due to the increased emissions from high-temperature combustions^{8,35}.

1.3 Sources for HNO₃ formation

The secondary pollutant HNO₃ is mainly formed in the atmosphere through the reaction of NO₂ with the OH• (hydroxyl radical) during daytime (reaction R3) and hydrolysis of dinitrogen pentoxide (N₂O₅) at night-time (reaction R4)³⁶:



Here M is an O₂ or N₂ molecule, which acts as third body that absorbs the excess energy. The scavenging of nitric acid gas in the atmosphere is reported as the dominant pathway for rain acidity³⁷. The sources and formation of HNO₃ include many reactions, and there is a clear correlation between HNO₃ concentration, wind speed, wind direction, temperature, solar intensity and concentration of other pollutants, including O₃ and peroxyacetyl nitrate³⁸⁻⁴⁰. Recent investigations at several European sites have shown that the highest HNO₃ concentrations are observed at urban sites in southern Europe during the summer³⁴.

1.4 Previous corrosion-related work with HNO₃

The magnitude of HNO₃-induced corrosion effects relative to other pollutants, such as SO₂, NO₂ or O₃, has not yet been quantified even though HNO₃ is potentially harmful to many materials. This is probably attributed to the chemical properties of HNO₃, e.g. its high tendency to absorb on surfaces, its relatively low airborne concentration and the lack of a commercial analytical instrument for measuring real-time concentration. This makes corrosion exposures in the laboratory difficult to perform, especially regarding control and monitoring of the actual HNO₃ concentration in the exposure chamber and measurement of the deposited amount on the sample. However, some HNO₃-related corrosion studies have been reported, dealing with the deterioration of calcareous stone materials⁴¹⁻⁴⁴. In all, the studies emphasize the importance of HNO₃ on the atmospheric corrosion of stones. HNO₃ reacts with the main constituent of marble and limestone, i.e. calcium carbonate (CaCO₃), and forms calcium nitrate, Ca(NO₃)₂, (reaction R5):



Like many other nitrate salts, calcium nitrate is highly water soluble and hygroscopic⁴⁴ and is easily washed from the surface during exposure.

Lipfert (1989) deduced an empirical dose-response function that includes HNO₃ for deterioration of limestone⁴⁵. This function correlates the mass loss of stone materials with the deposition rates of various pollutants and the pH of rain. Using Lipfert's dose-response function, Pantani et al. (1998) reported decreased mass loss of marble at a rural site in Italy, due to decreased SO₂ levels over the last decades, and increased mass loss due to increased HNO₃ levels during the same time period³⁵.

Apart from this study the only investigation that concerns the effect of HNO₃ on the corrosion of metals was presented by Cramer et al. in 1996⁴⁶. In their paper the authors proposed a dose-response function, which includes the effects of wet and of dry acid deposition on the corrosion rate of copper.

Partly in order to fill this gap of knowledge concerning the role of HNO₃, two international projects were initiated in the period 2001-2002, MULTI-ASSESS and RAPIDC. Within these projects extensive monitoring of HNO₃ levels at 29 European, 12 Asian and 4 African test sites were conducted together with exposure of materials. The corrosion effects of HNO₃ were also studied in artificial laboratory air for more well-controlled exposure conditions.

1.5 Overview of MULTI-ASSESS and RAPIDC projects

1.5.1 MULTI-ASSESS

In the beginning of 2002 a project started within the European Union Fifth Frame Work Programme (EU5FP) entitled MULTI-ASSESS, Model for Multi-Pollutant Impact and Assessment of Threshold Levels for Cultural Heritage. The main objective of the MULTI-ASSESS project was to develop a model of the combined effects of pollutants and climate parameters on deterioration and soiling of materials in cultural heritage objects. One year field exposures were conducted at 29 test sites in Europe of several metal, glass and stone materials. Pollution data were monitored using passive samplers for HNO₃, SO₂, NO₂, O₃ and particles. Also, climatic data on temperature, relative humidity, amount and pH of precipitation were obtained from nearby stations. Laboratory investigations were performed as an important complementary activity to field exposures. Especially the effects of HNO₃ were investigated since no similar study had been performed earlier. This laboratory study became the primary objective of the present doctoral study.

1.5.2 RAPIDC

During 2001-2004 the Swedish International Development Agency (SIDA) funded a Programme on Regional Air Pollution in Developing Countries (RAPIDC). The goal of this project was to transfer knowledge for corrosion damage assessment to institutes in Asia and Africa. For this purpose a network of 16 test sites was established in Asia and Africa and standard specimens of carbon steel, zinc, copper, limestone and paint coated steel were exposed at each of the sites in unsheltered positions. Similar to the MULTI-ASSESS project (see above) pollution data and climatic data were collected at each exposure site for developing dose-response functions. The second phase (2005-2008) of the RAPIDC Programme is still on-going.

Both MULTI-ASSESS and the first phase of RAPIDC were co-ordinated by the Swedish Corrosion Institute. The second phase of RAPIDC is now co-ordinated by the Corrosion and Metals Research Institute (KIMAB). Further details can be found elsewhere^{11,22,47}.

1.6 Purpose of the study

With the initiation of the MULTI-ASSESS project and the objective to investigate the effects of HNO₃ on degradation of materials through laboratory exposures, the basis for this doctoral study was established. Laboratory exposures provide detailed information on the relationship between environmental parameters in the corrosion process and their connection to corrosion effects of, e.g., pollutant and concentration. However, the test conditions often suffer from lack of realism. In order to establish the connection between environmental parameters and corrosion effects, laboratory investigations must be combined with field studies. Thus, another important part of this work was to combine laboratory with field investigations. The field data included exposure of the same materials and monitoring of important pollutants and environmental data within the RAPIDC as well as MULTI-ASSESS project. The aims of this doctoral work can be summarised as follows:

- Development of an experimental set-up for accelerated HNO₃ exposures of materials, which reproduces the most important outdoor exposure conditions.
- Development of a method for validation of the HNO₃ concentration within the laboratory exposures.
- Investigation of the corrosion effects of HNO₃ concentration, wind velocity, temperature, relative humidity and exposure time on copper.
- Investigation of the corrosion effects of HNO₃ on zinc and carbon steel.
- Comparison of the effects of HNO₃ and SO₂ on the atmospheric corrosion of copper, zinc and carbon steel when exposed to similar laboratory conditions.
- Comparison of the corrosion effects of HNO₃ on copper, zinc and carbon steel obtained during laboratory and field exposure conditions, respectively.

2. Experimental

2.1 Experimental set-up

The development of the chosen experimental set-up was carried out after considering several options. Many of these were rejected at early stages due to the complexity of the construction, high costs or insufficient safety during operation. One of the most promising alternatives was proposed by Ferm (2002)⁴⁸. This included a dynamic system with small fans in air pipes used previously for exposures of samples to ozone⁴⁹. The most important drawbacks of this concept, however, were difficulties in introducing the samples without disturbing the experimental conditions, achieving homogeneous HNO₃ deposition on both sides of the samples and difficulties to see the samples during the exposure. Also, the use of the denuder technique for concentration measurement, described in more detail elsewhere⁵⁰⁻⁵², was considered as time consuming.

The final experimental construction in this study was entirely made of quartz glass; Teflon was used in all connections and tubings with the exception of inlets in the aquarium where quartz glass was used (see Fig. 1).

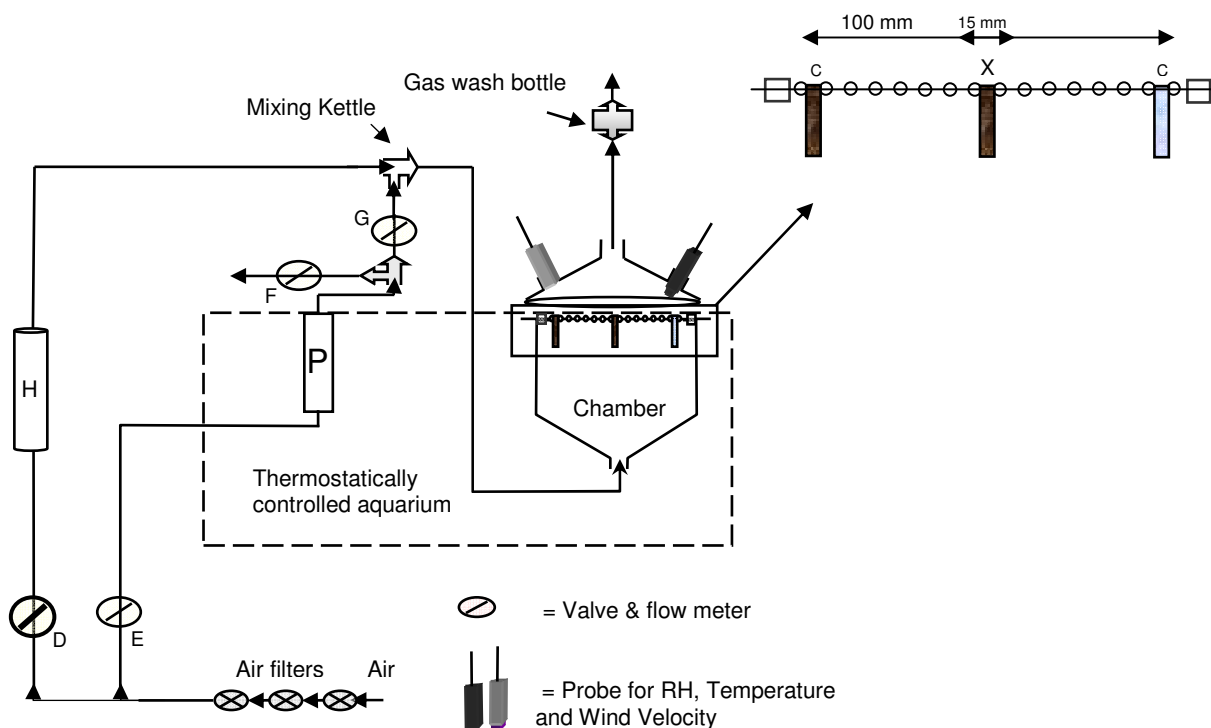


Fig. 1. Schematic view of the experimental set-up (see text).

After passing air filters, the purified and dried air was divided into two streams. One stream was bubbled into a bottle filled with ultra pure water and then directed to a glass coil surrounded by thermostated water (denoted H in Fig. 1). The desired relative humidity (RH) was achieved by changing the temperature of the water. The other stream, having a considerably lower flow rate, was used as a carrier for HNO₃ emitted from temperature controlled permeation tubes (denoted P in Fig. 1; Kin-Tek, LeMarque, TX) via a needle valve E (model P04/1, Kytölä Instrument). The needle valves F and G were made of Teflon (model T54/1, Kytölä) and used for changing the concentration of the gas by adjusting the flow up to a maximum of 15 cm³ min⁻¹. The valve D was used to control the exit flow from the chamber up to 2400 cm³ min⁻¹. The water filled aquarium was equipped with a digital thermostat and was used as the surrounding medium for the chamber to obtain a stable temperature, which also limits the operation of the humidifier.

The HNO₃ containing air was introduced into the chamber from the bottom, where the samples were suspended vertically on a glass rod at marked positions (C and X in Fig. 1). As HNO₃ is readily dissolved in water, the exit air from the chamber was directed into a gas wash bottle containing a known amount of ultra pure water. Thus, the hazardous and corrosive air could be cleaned from HNO₃ and the corresponding HNO₃ concentration could be estimated from the amount of nitrate in the gas wash bottle quantified by ion chromatography. The temperature and relative humidity in the chamber were measured with a Testo 645 instrument and the air velocity with an anemometer model Testo 425. These measurements were performed by probes introduced in the chamber via small openings in the lid.

In a comparative study of different tubing materials it was shown that the adsorbing ability of HNO₃ was the highest for glass surface and the smallest for Teflon^{53,54}. However, quartz glass was chosen since it is transparent and in comparison to Teflon, glass is highly non-permeable for gases. The adsorption was acceptable since the entire construction including the chamber, made of quartz glass, and all other connections and fittings were saturated within three days in dry air (see Fig. 2).

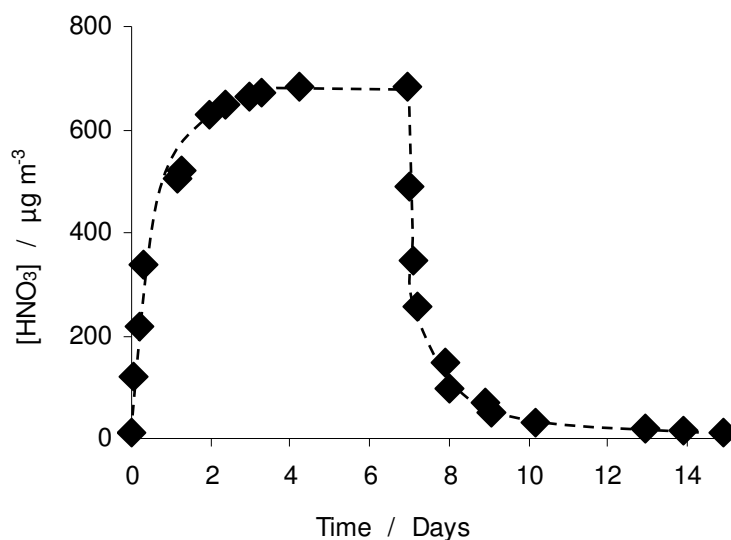


Fig. 2. *HNO₃ concentration in the chamber exit air at 0 % RH, 25 °C and 0.03 cm s⁻¹ air velocity as HNO₃ is introduced at day 0 and disconnected at day 7. The plateau reached indicates that the inside walls were saturated within three days.*

2.2 Difficulties, failures and modifications

The original idea to simulate and investigate the effects of wind velocity was to place four small plastic fans at the bottom of the chamber and therefore it was designed with a rather large dimension (~220 mm Ø). Although the turbulence of air due to the operating fans would make it virtually impossible to predict the direction of the flow, this method was considered as a good option for simulation of strong winds. An anemometer probe could be used to measure the approximate air velocity at the sample position. However, this method was unsuccessful as the plastic fans absorbed a huge amount of HNO₃. The fans were introduced inside the chamber after extensive Teflon coating and also plasma treatment, and exposed during six weeks at ppm levels of HNO₃. Neither of these treatments resulted in significant reduction in HNO₃ consumption of the fans.

One of the alternative methods, previously used by Tidblad and Leygraf (1995)⁵⁵, included a rotating arm introduced in the chamber on which samples could be suspended vertically. This method was considered as insufficient in order to achieve high enough air velocities. The option finally selected was to decrease the cross-section area of the chamber by introducing a massive Teflon block with small cells, on which samples could be suspended (see Fig. 3). Use of this method resulted in air velocities up to 35.4 cm s⁻¹, which was substantially higher than the 0.03 cm s⁻¹ when no Teflon block was used (see Fig. 1).

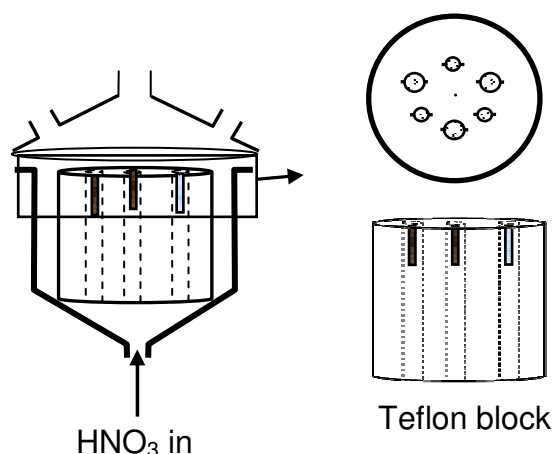


Fig. 3. Schematic view of the modified chamber for exposures with increased air velocity. A cylindrical Teflon block with six cells of varied diameters was used in order to decrease the cross-section area. Also, each cell could be closed with a Teflon seal to increase the air velocity in the other cells.

Another difficulty was to maintain a steady HNO_3 concentration in the chamber. The importance of RH fluctuations became evident as the HNO_3 concentration changed radically as the lid was opened for introduction or removal of the exposed samples. Not surprisingly, as the RH increased, a thicker water layer (adlayer) was formed on the surfaces. As these surfaces needed to be saturated, the HNO_3 concentration decreased dramatically for a short time in the chamber. On the other hand, after saturation of the adlayer, a decrease in RH resulted in a release of HNO_3 from the walls and an even more dramatic increase in HNO_3 . As an example, the decrease of RH from 82 % to 0 % resulted in instant increase of HNO_3 concentration in the exit air by an approximate factor of 20 (see Fig. 4).

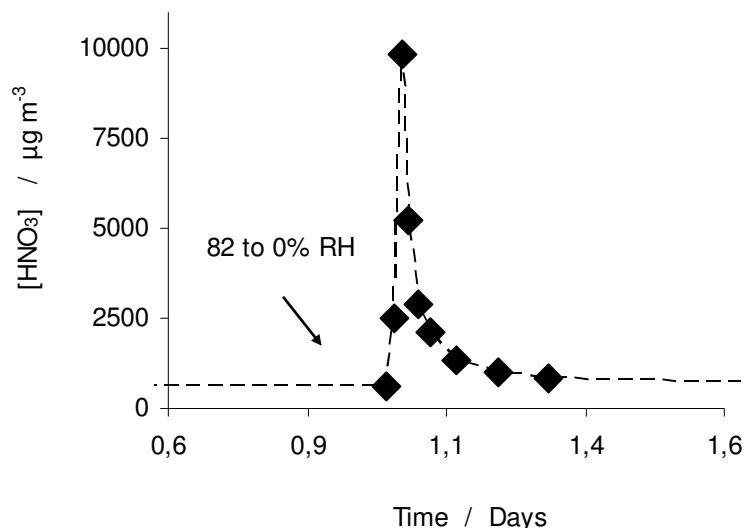


Fig. 4. Concentration changes of HNO_3 when RH is decreased from 82 % to 0 % at 25 °C and 0.03 cm s^{-1} air velocity.

Depending on the magnitude of the RH fluctuations, the concentration in the system was stabilized within one day. Whether this time is of importance depends on the total exposure time. However, for understanding the mechanism of the initial stage of corrosion, it was considered important to remove this artefact.

A new method was therefore developed to introduce the samples via small openings in the lid, i.e. without opening the entire lid. Thus, the RH was kept constant (see Fig. 5) and the consumption of HNO_3 in the chamber could be attributed to the samples only.

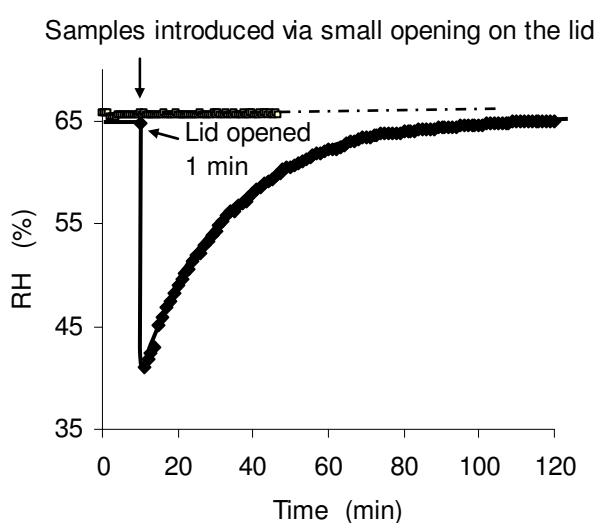


Fig. 5. RH variations in the chamber when the entire lid is opened for 1 min (the solid line) and when samples are introduced via a small opening in the lid (the dashed line).

2.3 HNO₃ analysis

The HNO₃ concentration, [HNO₃], in the chamber was obtained from nitrate analysis of dissolved HNO₃:

$$[HNO_3] = \frac{C_{NO_3^-} \times V \times M_{HNO_3}}{M_{NO_3^-} \times F \times t} \quad (\text{eq. 1})$$

where V is the volume of ultra pure water in the gas wash bottle (see Fig. 1), M is the molar mass, F is the air flow rate, and t is the sampling time. The analysis of nitrate by measuring the concentration, C_{NO₃⁻}, was performed by an ion chromatograph (IC), model Metrohm with 733 IC Separation Center, 709 IC pump and 752 Pump Unit. The column chosen was of model 6.1006.5X0 Metrosep A Supp 5. The prepared eluent was 3.2 mmol L⁻¹ Na₂CO₃ and 1.0 mmol L⁻¹ NaHCO₃ in 5 % acetone, with flow rate 0.70 ml min⁻¹. Detection was done with an electric conductivity detector model Metrohm 732 IC Detector. Reproducibility of IC nitrate analysis was tested with prepared standards and the differences in repeated sample analyses of the same sample were lower than 5 %.

In order to verify the HNO₃ concentration measurements, the permeation rate of the permeation tube was monitored gravimetrically and compared to the IC concentration measurements (see Fig. 6). A good agreement was observed between these two methods.

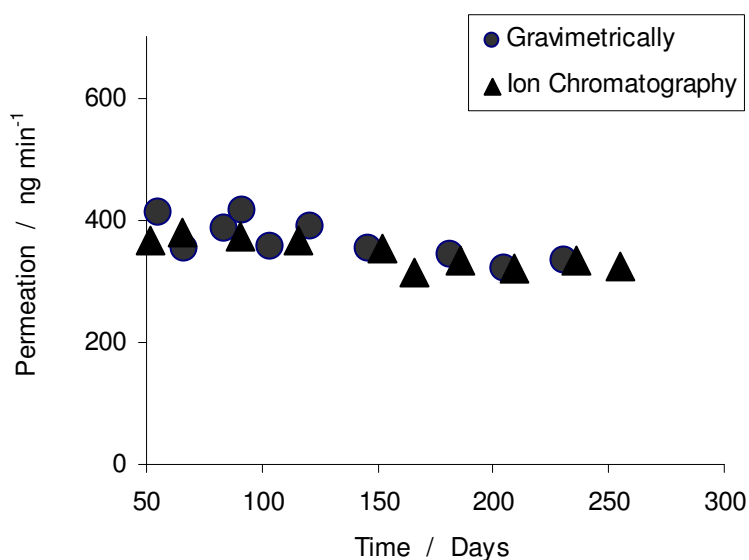


Fig. 6. Permeation of HNO₃ from a permeation tube measured gravimetrically and compared with IC analysis.

2.4 Preparation of samples

The specimens were cut from approximately 1 mm thick sheets to a total geometrical area of 10 cm² (1.0 cm × 5.0 cm). Copper and zinc sheets were of 99.9 % purity and the carbon steel sheet contained ≤ 0.12 % carbon (C), ≤ 0.60 % manganese (Mn), ≤ 0.05 % sulphur (S) and ≤ 0.5 % phosphor (P). The samples were polished to 2400 mesh in ethanol and washed in acetone using ultrasonic agitation. Immediately after this treatment, the samples were dried using a hairdryer and transferred to a desiccator 1 to 4 days before exposure in the chamber.

The deposition of HNO₃ on a perfect (ideal) absorbent was measured using a sodium hydroxide (NaOH) impregnated Munktell filter paper of the same dimensions as the metal samples. The experiments conducted included two metal samples and one filter paper. The filter paper was positioned symmetrically to one metal sample, as is shown in Fig. 1, to minimize the effects of inhomogeneous flow and deposition of HNO₃. In experiments with increased air velocity by use of the Teflon block (see Fig. 3), each sample was suspended in one cell.

2.5 Estimation of HNO₃ deposition

The total deposition of HNO₃ on the samples during each laboratory exposure, m_{chamber} (μg), was determined by use of the following parameters (see eq. 2): the air flow rate (F) in m³ s⁻¹, the exposure time (t) in s, the HNO₃ concentration prior to exposure and the average concentration during the exposure in μg m⁻³, $[\text{HNO}_3]_s$ and $[\text{HNO}_3]_e$ respectively. Fig. 7 shows a typical trend of concentration during exposure of samples.

$$m_{\text{chamber}} = F \times t \times ([\text{HNO}_3]_s - [\text{HNO}_3]_e) \quad (\text{eq. 2})$$

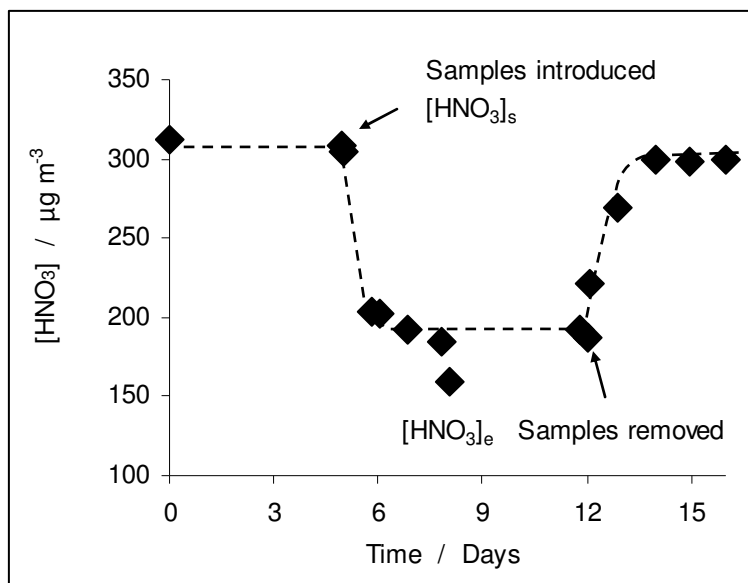


Fig. 7. HNO₃ concentration of the exit air when one filter and two copper samples are exposed at 63 % RH, 25 °C and 0.03 cm s⁻¹ air velocity.

For determination of the deposition velocity (V_d) of HNO_3 on the ideal absorbent and the metal samples the following procedure was conducted. By leaching the filter in ultra pure water the nitrate concentration could be measured and the corresponding HNO_3 deposition on the filter, m_{filter} (μg), recalculated. However, it was not possible to reliably measure the amount of deposited HNO_3 on the metal samples independently although several different leaching solutions were tested. Thus, the HNO_3 deposition on a metal sample, G_{metal} ($\mu\text{g cm}^{-2}$) was estimated indirectly as:

$$G_{\text{metal}} = \frac{m_{\text{chamber}} - m_{\text{filter}}}{2A} \quad (\text{eq. 3})$$

where $2A$ (cm^2) is the total surface area of two metal samples ($2 \times 10 \text{ cm}^2$). The V_d of HNO_3 (cm s^{-1}) can then be calculated as:

$$V_d = \frac{G}{C \times t} \quad (\text{eq. 4})$$

where G ($\mu\text{g cm}^{-2}$) is the HNO_3 deposition on the filter or metal and C is the HNO_3 concentration in $\mu\text{g cm}^{-3}$.

2.6 Gravimetical analysis

The mass gain and mass loss were determined by weighing the specimens prior to exposure, after exposure and after removal of the corrosion products by using adequate pickling solutions (see below). The mass gain represents the total amount of other elements than the base metal, e.g. hydrogen, nitrogen and oxygen, which have been incorporated into the corrosion layer or deposited on the surface. The mass loss represents the total amount of the base metal that has been transformed to a corrosion product during the exposure. The pickling solutions for the metals were as follows; copper was pickled in amidosulfonic acid ($\text{H}_3\text{NO}_3\text{S}$), zinc in saturated glycine ($\text{C}_2\text{H}_5\text{NO}_2$) and carbon steel in Clark's solution. Small amounts of bulk metal were removed during the pickling procedure, which were corrected for by using the same amount that was removed when pickling unexposed metal samples.

2.7 Corrosion product analysis

For identification of crystalline corrosion products formed on laboratory exposed samples an XRD (X-ray diffraction) instrument equipped with a Guiner-Hägg camera was used. Fourier transfer infrared spectroscopy (FT-IR) using a Biorad FTS175C spectrometer equipped with a broad-band mercury cadmium telluride (MCT) detector was used for verification of XRD results and identification amorphous components. In some cases IC analysis of water soluble ions, mass gain and mass loss analyses of laboratory exposed samples were conducted in order to provide further information regarding corrosion products.

2.8 Field studies

The methodology for field exposures and the exposure rack have been described more in detail elsewhere²² (paper VII). The field exposures and results in themselves are not the subject of this thesis, but since they are used in an important comparison with the laboratory exposures (paper V) a summarized description of the methodology is given below.

The test specimens of copper, zinc and carbon steel were cut to areas of $150 \times 100 \text{ mm}^2$ and thickness of 1-2 mm. Each plate was degreased, dried and weighed before exposure on a wooden frame, facing south at the northern hemisphere, or north at the southern hemisphere at an angle of 45° to the horizontal (see Fig. 8). The corrosion rate and product analyses of field exposed metals were similar to those exposed in the laboratory (see above).



Fig. 8. Metal plates mounted on a typical exposure rack made of wood, facing south at the northern hemisphere, or north at the southern hemisphere, at an angle of 45° to the horizontal. The plates are fastened to the rack with stainless steel screws using plastic insulators.

3. Results and discussion

It is evident that a pollutant cannot be harmful to a material unless it is deposited on the surface. The deposition velocity, which is a mass transfer coefficient and not a traditional velocity, of a pollutant depends mainly on its chemical properties, the material, pH in the liquid film on the metal surface, the concentration of the pollutant in the surrounding atmosphere and the air velocity⁵⁶. Smith et al. (2000) reported HNO₃ dry deposition rates to be highly sensitive to both wind speed and concentration⁵⁷. Under ambient conditions these two parameters were shown to be more important for deposition of HNO₃ than for other gases, e. g. NO₂, O₃, SO₂ or NH₃.

The surface moisture acts as a natural sink for pollutants. Thus, as the water soluble and acidic gas HNO₃ is dissolved in the adlayer an electrolyte is formed resulting in the formation of nitrate salts through proton exchange (see introduction). According to Phipps and Rice (1979) for the aqueous layer to approach bulk properties, the number of water monolayers on the metal surface must be thicker than three¹⁵, which is reached at approximately 60 % RH and 20 °C¹². However, increased relative humidity favours the condensation of moist, but whether condensation will occur also depend on the temperature, the surface characteristics and the properties of the corrosion product¹.

The influence of temperature on the corrosion rate of metals is two-fold. On one hand, a high temperature results in faster drying of the humid layer and can therefore reduce the corrosion rate. On the other hand, an increased temperature accelerates most chemical processes, including the corrosion reactions.

The corrosion rate of clean metal surfaces is high initially, as the whole area is available for attack, but the rate normally slows down¹.

The role of these briefly described parameters; concentration, air velocity, exposure time, relative humidity and temperature on the corrosion rate of laboratory exposed copper in HNO₃-containing air will be presented in the following (Paper I, II and III). This continues with a comparison of corrosion effects of HNO₃ on copper, zinc and carbon steel (Paper IV), a comparison of corrosion effects of HNO₃ to those of SO₂ on the same metals (Paper IV), and finally, a comparison of laboratory and field exposed metals (Paper V).

In the text below, when no additional detail is given, the expression “laboratory exposures” refers to an exposure during 7 days at 65 % RH, 25 °C, 0.03 cm s⁻¹ air velocity and 100-460 µg m⁻³ HNO₃. The concentration given for each laboratory experiment is based on an

average of the input concentration, measured as the concentration before exposure, and the output concentration, measured during exposure (see Fig. 7). Field exposure refers to one-year exposure of the samples as described in section 2.8.

It should be mentioned that the relatively high HNO_3 concentrations in the laboratory exposures, compared to typical ambient levels, were used in order to obtain measurable corrosion rates and to provide comparable conditions as those in similar investigations of corrosion effects of other corrosive pollutants. In contrast, the air velocity used in the laboratory exposures is far below average outdoor air velocity. However, as will be presented later (section 3.4), the extrapolation of laboratory results to outdoor conditions agrees well with field data.

3.1 HNO_3 effects on copper (Paper I, II and III)

Extensive laboratory studies on the influence of the important parameters HNO_3 concentration, air velocity, temperature and relative humidity was performed on copper since copper is a widely used metal and is included both in the MULTI-ASSESS and RAPIDC projects, as is zinc and carbon steel. Also, nitrate has been identified in copper corrosion products in contrast to field exposed zinc and carbon steel, where the presence of nitrate in the corrosion products is rare^{58,59}.

3.1.1 Effects of concentration

The influence of HNO_3 concentration on the initial atmospheric corrosion of copper was investigated at 65 % RH, 25 °C and 0.03 cm s^{-1} air velocity. Similar to the impregnated filter, i.e. the ideal absorbent for HNO_3 , the deposition rate on copper was proportional to the HNO_3 concentration. Also, the mass gain of copper samples showed a linear dependence with HNO_3 concentration up to 400 $\mu\text{g m}^{-3}$ (Fig. 9).

It should be noted that the fitted line in Fig. 9 does not pass through the origin and intercepts the vertical axis at about 1.0 $\mu\text{g cm}^{-2} \text{d}^{-1}$, which can probably be attributed to the formation of cuprite (Cu_2O). Combined information obtained by XRD, FT-IR, IC and gravimetric analyses showed that the main constituents of the copper corrosion product obtained in the laboratory were the basic copper nitrate, gerhardtite ($\text{Cu}_2(\text{NO}_3)(\text{OH})_3$) and, to a smaller extent Cu_2O .

The linear increase in HNO_3 deposition and mass gain of copper with HNO_3 concentration demonstrates the high solubility in water and reactivity of HNO_3 , as will be discussed further below.

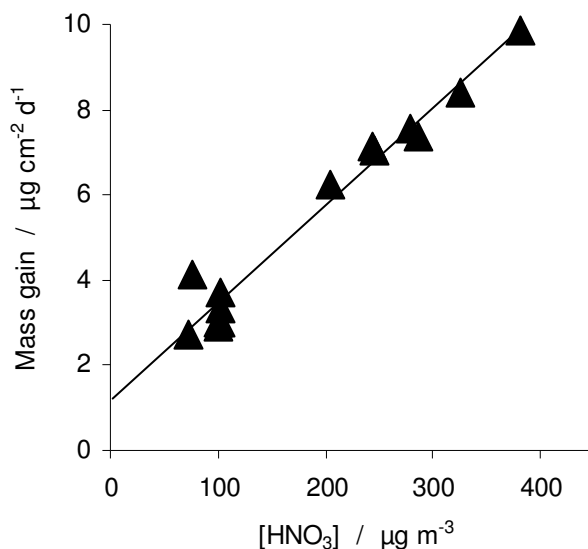


Fig. 9. Mass gain of copper versus HNO_3 concentration at 65 % RH, 25 °C and 0.03 cm s⁻¹ air velocity.

3.1.2 Effects of air velocity

The influence of air velocity was investigated between 0.03-35.4 cm s⁻¹. The deposition velocity (V_d) of HNO_3 on an impregnated filter and copper (eq. 4) at different air velocities is illustrated in Fig. 10. The V_d of HNO_3 on the filter increased linearly with the air velocity up to 35.4 cm s⁻¹. The V_d of HNO_3 on copper, however, was similar to that on the filter below 11.8 cm s⁻¹, indicating mass transport limiting conditions but somewhat lower at 35.4 cm s⁻¹. The same trend was observed for the mass gain of copper. Thus, up to 11.8 cm s⁻¹ mass transport in the gas phase is rate limiting, but at higher air velocities (35.4 cm s⁻¹) mass transport is not the only rate-limiting factor. In a previous study, Volpe and Peterson (1989) investigated the effects of hydrogen sulfide (H_2S) and air velocity on the corrosion rate of copper⁶⁰. In agreement to results presented here, the mass gain increased with air velocity up to 20 cm s⁻¹, but above 20 cm s⁻¹ the mass gain decreased in experiments with H_2S , whereas the mass gain continued to increase, although slower, in our experiments with HNO_3 .

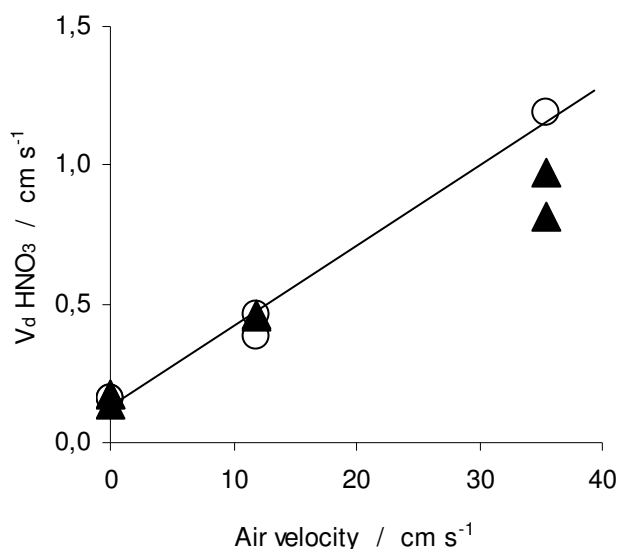


Fig. 10. V_d of HNO_3 on impregnated filter (circles) and copper (triangles) versus air velocity at 65 % RH, 25 °C, and $325 \mu g m^{-3} HNO_3$.

In order to understand the nature of the flow, laminar or turbulent, the Reynolds number (Re) was calculated by the following well known equation^{26,61}:

$$Re = \frac{l \times u}{\nu} \quad (\text{eq. 5})$$

where l is the length of the sample parallel to the air flow (5.0 cm), u is the average air velocity and ν is the kinematic viscosity of air ($0.143 \text{ cm}^2 \text{ s}^{-1}$). The flow is turbulent if Re is above 2000. In experiments here Re is at most 1240 and therefore the flow should be laminar, which appears to be uncertain for reasons given below. The thickness of the boundary layer, δ , was calculated by use of the equation:

$$\delta = \frac{D_0}{V_d} \quad (\text{eq. 6})$$

where D_0 is the HNO_3 diffusion coefficient ($0.11 \text{ cm}^2 \text{ s}^{-1}$)^{62,63} and V_d of HNO_3 at 35.4 cm s^{-1} is 1.2 cm s^{-1} (see Fig. 10). The δ obtained here is 0.10 cm and is, compared to δ given by Volpe and Peterson (1991)²⁶, approximately 0.5 cm, considerably lower. Also, the V_d should according to Volpe and Peterson (1991) be proportional to the square root of air velocity for laminar flow conditions. This is not applicable herein, where the V_d of HNO_3 increased linearly with air velocity. Thus, it is more likely that the design of the chamber gives rise to some turbulent conditions.

The highest wind velocity simulated here is at most 35.4 cm s^{-1} , which is far below outdoor conditions. Considering V_d to be affected by air and surface resistance, $V_{d,air}$ and $V_{d,surf}$, respectively, it can be expressed as

$$\frac{1}{V_d} = \frac{1}{V_{d,air}} + \frac{1}{V_{d,surf}}. \quad (\text{eq. 7})$$

Assuming a linear relation between V_d and air velocity, as described above, and extrapolating the data presented in Fig. 10 to an outdoor air velocity of 10 m s^{-1} the V_d of HNO_3 on copper is calculated to 3.2 cm s^{-1} , which is within the outdoor levels reported in the literature for other absorbing surfaces^{27,64-67}.

3.1.3 Effects of exposure time

The corrosion kinetics of copper exposed to HNO_3 was examined after 2, 7 and 14 days. Assuming that the only corrosion products formed on laboratory exposed copper are gerhardtite ($\text{Cu}_2(\text{NO}_3)(\text{OH})_3$) and cuprite (Cu_2O), the mass gain and mass loss of exposed samples were combined in order to estimate the amount of copper consumed due to gerhardtite or cuprite (Fig. 11). The mass gain due to Cu_2O , relative to $\text{Cu}_2(\text{NO}_3)(\text{OH})_3$, is very low. However, after 2 days of exposure the amount of copper consumed by Cu_2O formation and by $\text{Cu}_2(\text{NO}_3)(\text{OH})_3$ formation is nearly the same. The amount related to Cu_2O formation decreased substantially already after 7 days. Also, the total mass gain slowed down after 14 days, which can be attributed to the increasing thickness, constraining the transport through the corrosion layer.

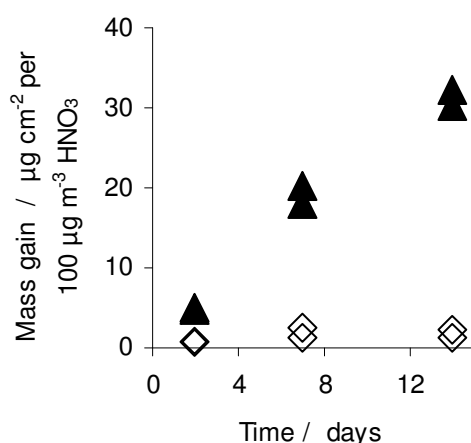


Fig. 11. Total mass gain of copper (triangles) and corresponding mass gain due to Cu_2O formation (squares) versus the exposure time at 65 % RH, 25 °C, 0.03 cm s^{-1} air velocity and sub-ppm levels of HNO_3 .

3.1.4 Effects of temperature

The influence of temperature was tested in the range +15 and +35 °C at 65 % RH, 0.03 cm s⁻¹ air velocity and sub-ppm levels of HNO₃. The mass analysis of exposed copper showed a minor decrease of cuprite in the corrosion layer with increased temperature. However, no significant change in the total mass gain or in V_d of HNO₃ could be observed at varying temperature. In all, the corrosion rate of copper was little affected by a raise of temperature from 15 °C to 35 °C at 65 % RH, which agrees well with other results on copper reported in the literature^{68,69}.

3.1.5 Effects of relative humidity

In experiments with HNO₃ the corrosion rate of copper was significant even at 20 % RH, 25 °C and low air velocity (0.03 cm s⁻¹). Up to 40 % RH the mass gain of copper increased relatively little (<1 µg cm⁻² d⁻¹ per 100 µg m⁻³ HNO₃) while at 65 % RH it increased to nearly 3 µg cm⁻² d⁻¹ per 100 µg m⁻³ HNO₃. A further increase from 65 to 85 % RH did not have any significant effect on the mass gain. A similar trend was observed for the V_d of HNO₃ on copper (see Fig. 12).

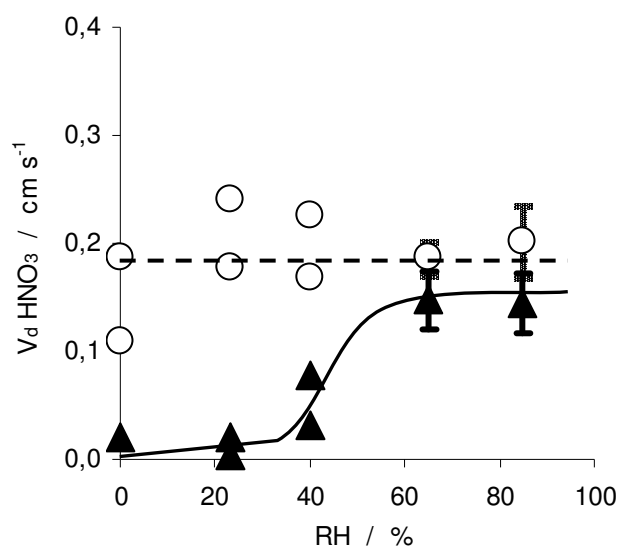


Fig. 12. V_d of HNO₃ on filter (circles) and copper (triangles) versus relative humidity upon exposure to sub-ppm levels of HNO₃, 25 °C and 0.03 cm s⁻¹ air velocity. Error bars show the standard deviation of at least three samples. The solid line is a guide to the eye.

As was discussed earlier, an adlayer thicker than three monolayers has properties that approach those of bulk water and this is obtained at approximately 60 % RH (see Table 2). At such conditions the adlayer is likely to act as a perfect sink for HNO₃ due to its high solubility and reactivity. And as the surface resistance, $V_{d,surf}$, decreases (see eq. 7) the total V_d increases. At 65 % RH bulk properties of water are reached and, hence, the V_d of HNO₃ on the copper surface reaches a plateau.

Table 2

Approximate number of water monolayers on different metal and alloy surfaces, including gold, cobalt, nickel, iron and nickel-iron alloys at 25 °C versus RH.

RH (%)	Number of monolayers
20	1
40	1.5-2
60	2-5
80	5-10

Data from ref. 27.

3.2 Comparison of HNO₃ effects on copper, zinc and carbon steel (Paper IV)

This section will present a comparison of the corrosion effects of HNO₃ after briefly summarising the results on corrosion of zinc and carbon steel exposed to HNO₃.

XRD confirmed the presence of the basic zinc nitrate $Zn_5(NO_3)_2(OH)_8 \times 2H_2O$ on laboratory exposed zinc. The same compound was identified by Oesch and Faller (1997)⁷⁰, who exposed zinc to ppm levels of NO₂ and 90 % RH, and suggested the uptake of NO₂ to be attributed to the adsorption of HNO₃ formed in the gas phase (see section 1.3).

The corrosion effect of laboratory exposed carbon steel was higher than that of copper or zinc. Clearly visible rust islands were observed after less than one day of exposure to 390 $\mu\text{g m}^{-3}$ HNO₃ at 65 % RH, 25 °C and 0.03 cm s^{-1} . In Fig. 13 a representative part of a sample exposed for two weeks is shown. XRD analysis of samples taken from laboratory exposed carbon steel did not show any occurrence of nitrates. However, as nitrate was identified on the same samples by FT-IR analysis, the formed iron nitrate was most likely amorphous.

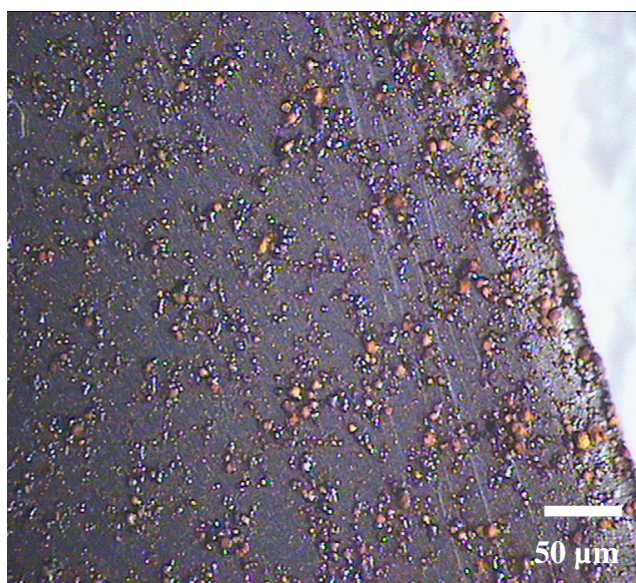


Fig. 13. Nitrate salts formed on a carbon steel sample exposed for two weeks to sub-ppm levels of HNO₃ at 65 % RH, 25 °C and 0.03 cm s^{-1} .

The air velocity is highest at the edges of the sample. Since the corrosion is mainly mass transport dependent on laboratory exposed carbon steel (Fig. 13), zinc and copper (cover figure), the largest amount of corrosion products were formed at the edges of each sample.

These were loosely adherent to the base metal and readily removed from the metal surface. Thus, it is evident that these corrosion products may not be able to protect the metal from further corrosion.

The V_d of HNO_3 on all metals at 65 % RH, 25 °C and low air velocity was at least 70 % of the V_d of HNO_3 on an ideal absorbent. Similar to the corresponding corrosion rate, the V_d of HNO_3 on these metals remained nearly unchanged between 65 and 85 % RH. This indicates that the maximum HNO_3 deposition on these metals is obtained already at 65 % RH, which coincides with conditions for forming an adsorbed layer with bulk water properties, as discussed above.

The high deposition of HNO_3 on the metals resulted in high corrosion rates. According to Leygraf and Graedel (2000)¹² the amount of adsorbed water on a metal depends on several surface properties, including the density of defects on the solid surface and its hydrophilic and hydrophobic properties. Furthermore, the authors reported that in comparison to copper and zinc, carbon steel is the metal most sensitive to relative humidity. In exposures to HNO_3 -induced air the highest mass loss of the three metals was observed for carbon steel (see Fig. 14).

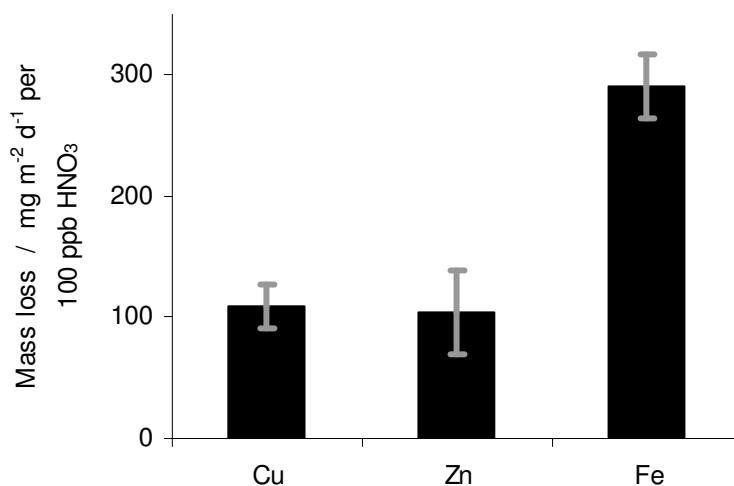


Fig. 14. Mass loss of copper, zinc and carbon steel exposed to sub-ppm levels of HNO_3 at 65 % RH, 25 °C and 0.03 cm s^{-1} air velocity. Error bars show the standard deviation of at least three samples.

3.3 Comparison of HNO₃ effects relative to SO₂ (Paper IV)

In the field of atmospheric corrosion it is well known that synergistic corrosion effects of several pollutants, e.g. SO₂, NO₂ or O₃, on metals are present. Reports have indicated that the corrosivity of a combination of SO₂ and O₃ on copper and zinc was far greater than that of SO₂, NO₂ or O₃ separately^{20,71}. Johansson (1984) reported the mass gain of carbon steel to be 30 times higher in exposure to a combination of SO₂ and NO₂ than when exposed to SO₂ alone¹⁰. However, results from this study show that the corrosion rate of metals exposed to HNO₃ alone was even higher. The relative corrosivity of HNO₃, as a single gas, compared to SO₂ or SO₂ in combination with NO₂ or O₃ is illustrated in Fig. 15. It is highest for zinc followed by copper and carbon steel. The relatively high corrosivity of HNO₃ is due to its water solubility which is far above that of SO₂ or NO₂ (see Table 1), resulting in a more acidic electrolyte.

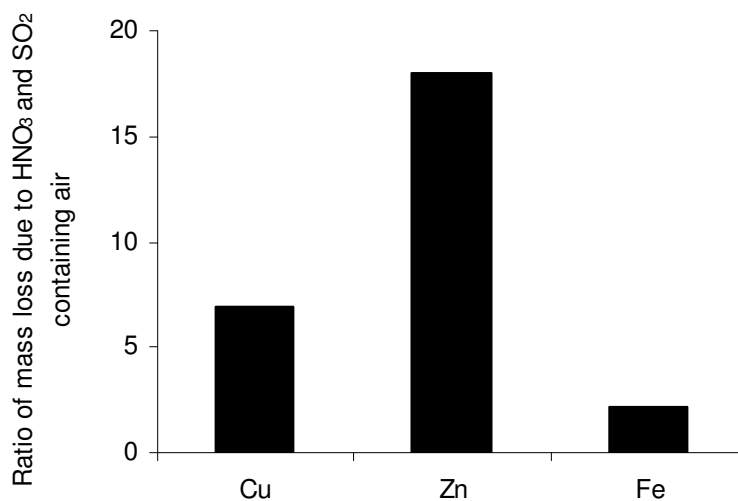


Fig. 15. Ratio of HNO₃- and SO₂-induced mass losses. HNO₃-induced mass losses are based on exposures at 65 % RH, 25 °C and 0.03 cm s⁻¹ air velocity. SO₂-induced mass losses are based on exposures to SO₂ containing air at 70 % RH for copper and zinc, and 90 % RH for carbon steel, 25 °C and a minimum of 0.3 cm s⁻¹ air velocity.

3.4 Comparison of laboratory and field data (Paper V)

FTIR analyses were conducted on laboratory and field exposed metals in order to identify possible occurrences of nitrate. Nitrate was found on all laboratory exposed samples (section 3.2) and field exposed copper and zinc.

The basic nitrates, e.g. gerhardtite, have in general low water solubilities⁷² and in contrast to carbon steel, basic nitrates have been reported as a constituent in corrosion products of copper and zinc^{59,70,73}. In the present investigation, nitrate was found on field exposed copper (see Fig. 16) and zinc. The relative nitrate peak was stronger for a sample taken from the back side, i.e. the side facing the ground, compared to the front side. This is not surprising, as the front side, i.e. the side facing the sky, is more affected by rain, which can also be acidic and dissolve basic nitrates.

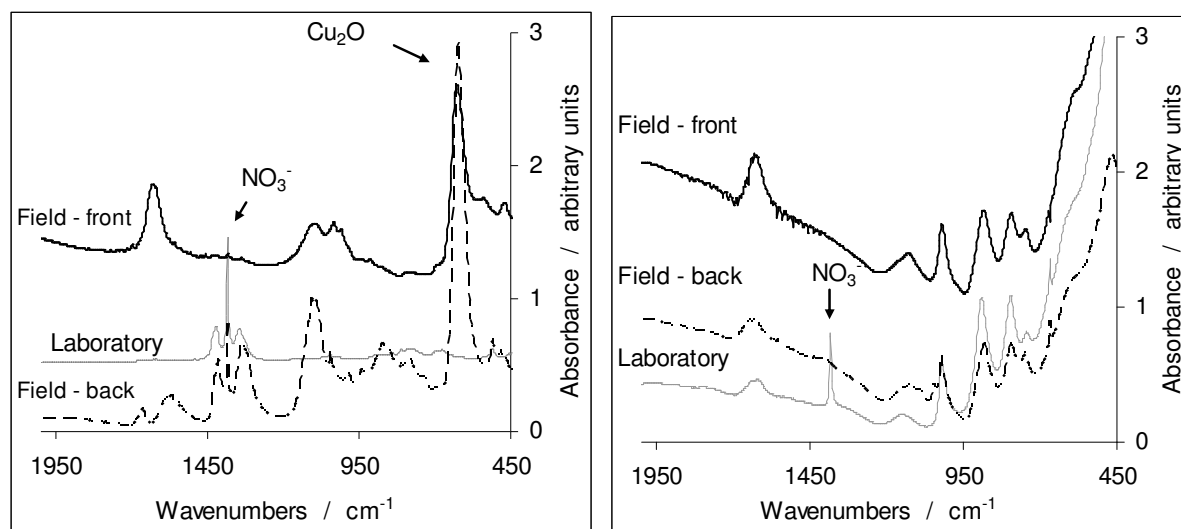


Fig. 16. FTIR spectrums of corrosion products from copper (left) and carbon steel (right). Exposures in laboratory (grey line) and front side and back side of the samples after field exposure at the test site in Kuala Lumpur (solid line and dashed line, respectively).

The lack of a nitrate peak on the FTIR spectra of field exposed carbon steel (see Fig. 16) does not exclude the formation of nitrates as a constituent of carbon steel corrosion products. In fact, the relatively high V_d of HNO₃ on laboratory exposed samples (section 3.2) suggests that iron reacts with HNO₃. Some authors have reported the presence of an iron nitrate, possibly Fe(NO₃)₃ × 9H₂O or Fe(NO₃)₂ × nH₂O, on carbon steel exposed in the field and in the laboratory^{4,12}. These corrosion products are not basic and it is most likely that insignificant amounts of nitrates are retained on field exposed carbon steel. It should be

mentioned that the field samples used here were exposed in Kuala Lumpur in Malaysia, a site with relatively long periods of heavy rain. Thus, it is possible that iron nitrate can be found on the back side of other samples exposed at sites with less intense precipitation than Kuala Lumpur.

The mass losses of field exposed copper, zinc and carbon steel at different HNO₃ doses are presented in Fig. 17. In order to enable a comparison between field and laboratory exposures, the V_d of HNO₃ obtained on laboratory exposed metals were extrapolated to an estimated average field wind velocity of 3.6 m s⁻¹ based on the geographical co-ordinates of the test sites and climate normals for the period 1961-1990 on a 19 minute grid⁷⁴. The extrapolated V_d of HNO₃ combined with the stoichiometry of the corrosion products were used to calculate the mass loss (ML) by the following equation:

$$ML = [HNO_3] \times V_{d\ HNO_3} \times t \times \frac{n \times M_{Me}}{M_{HNO_3}} \quad (\text{eq. 8})$$

where [HNO₃] is the HNO₃ concentration, t is time of exposure, M_{Me} is the molar mass of the exposed metal, M_{HNO₃} is the molar mass of HNO₃ and n is the molar ratio of nitrate and metal in the corrosion product. As an example, at a wind velocity of 3.6 m s⁻¹ the extrapolated V_d of HNO₃ on copper is 2.65 × 10⁻² m s⁻¹, t is 31536000 s (1 year), n for gerhardtite, Cu₂(NO₃)(OH)₃, is 2÷1, M_{Cu} and M_{HNO₃} is 63.6 g mol⁻¹ and 63.0 g mol⁻¹ respectively. Thus, ML of copper at 2.5 × 10⁻⁶ g m⁻³ HNO₃ is 4.2 g m⁻². The extrapolated ML at varied HNO₃ doses are represented as dashed lines in Fig. 17. Furthermore, in a dose-response function based on statistical analysis of field data Tidblad et al. (2004)⁴⁷ found a dependence between HNO₃ and zinc corrosion (eq. 9). This HNO₃ effect on the mass loss of zinc is presented as a solid line in Fig. 17.

$$ML = 3.53 + 0.471[SO_2]^{0.22} e^{0.018RH+f(T)} + 0.041\text{Rain}[H^+] + 1.37[HNO_3] \quad (\text{eq. 9})$$

$$f(T) = 0.062(T-10) \text{ when } T < 10^\circ\text{C}, f(T) = -0.021(T-10) \text{ otherwise}$$

where ML is the corrosion rate in g m⁻², [SO₂] and [HNO₃] is the concentration in µg m⁻³, RH is the relative humidity in %, rain is the amount of precipitation in mm, [H⁺] is the H⁺ concentration in mg L⁻¹ and T is the temperature in °C. From this equation it is evident that HNO₃ has a significant effect on the atmospheric corrosion of zinc.

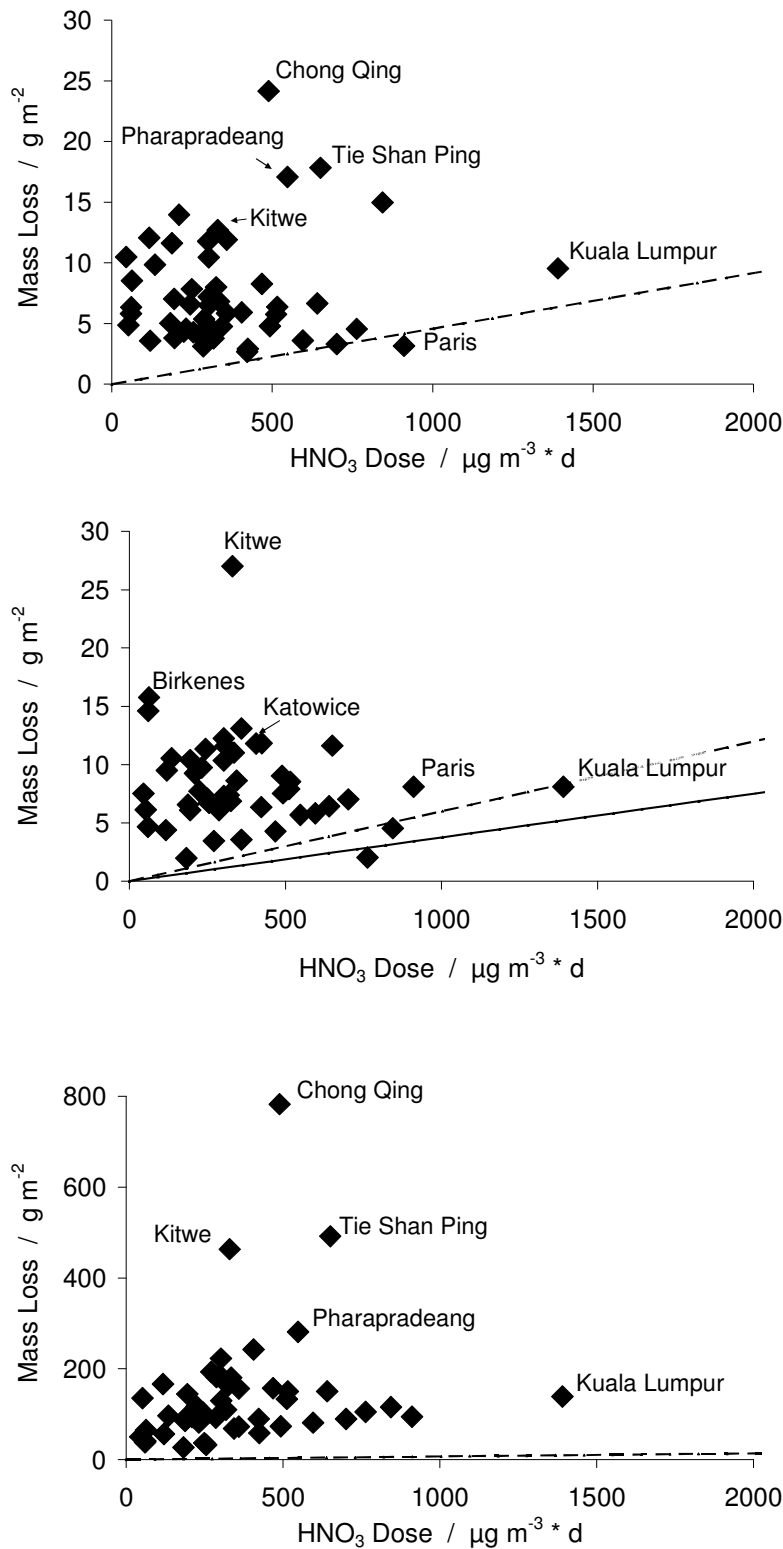


Fig. 17. Mass loss of copper (upper), zinc (middle) and carbon steel (lower) versus the HNO_3 dose. Data from 1 year field exposures are presented as squares and extrapolated laboratory experiments are included as a dashed line. The solid line in the zinc diagram represents the HNO_3 coefficient given in a dose-response function based on a statistical analysis of field data from the MULTI-ASSESS project⁴⁷ (eq. 9).

It is evident that HNO_3 results in a considerable part of the total corrosion effect on copper and zinc, but not of that on carbon steel. The extrapolated mass losses based on laboratory exposures are below nearly all field exposed samples, which is attributed to the presence of other corrosive pollutants in the ambient atmosphere, e.g. SO_2 , NO_2 and O_3 . The largest differences between extrapolated and field mass losses are for sites with high SO_2 concentration, e.g. Chong Qing and Tie Shan Ping in China, Kitwe in Zambia and Phrapradaeng in Thailand. In contrast, the mass loss of copper and zinc exposed at sites with relatively high HNO_3 and low SO_2 concentrations show a good fit to the laboratory extrapolated data. Among these sites are Kuala Lumpur in Malaysia and Paris in France. Also, the relatively good agreement between the extrapolated zinc mass loss and the dose-response function independently derived from a statistical analysis of field data shows that the present method to simulate the corrosion effects of HNO_3 was successful.

The relatively low corrosion effect of HNO_3 on carbon steel (see Fig. 17), compared to other corrosion stimulators, does not imply that carbon steel is less sensitive to HNO_3 than copper or zinc in absolute terms. However, carbon steel has a possibility to form passivating film at relatively low pH values, such as those induced by dissolved HNO_3 . Also, as was shown in the laboratory investigations, relative to a SO_2 -induced atmosphere, carbon steel showed the least sensitivity to HNO_3 , which again agrees well with the results presented in this section.

In all, although the ambient HNO_3 concentration is typically lower than SO_2 , the good agreement between extrapolated laboratory exposures and field data emphasizes the importance of HNO_3 on the atmospheric corrosion of copper and zinc.

4. Concluding remarks

The overall aim of this doctoral work has been to explore the role of HNO₃ in the atmospheric corrosion of three important metals, copper, zinc and carbon steel. HNO₃ is a gaseous constituent that finds increasing importance in many countries of the industrialized world, mainly because of the decreasing concentration of SO₂. The work includes both laboratory and field exposures. The main part has been devoted to the successful development and use of a method for laboratory exposures in HNO₃-containing atmosphere. A major experimental obstacle to overcome has been the high tendency of HNO₃ to absorb on humidified glass surfaces and other materials in the exposure chamber.

At sub-ppm concentrations of HNO₃ the deposition velocity of the gas is significant already at 20 % relative humidity (RH), 25 °C and an air velocity of 0.03 cm s⁻¹. When successively increasing RH, the deposition velocity increases dramatically between 40 and 65 % RH, and reaches a level close to that of an ideal absorbent for HNO₃. The same tendency is seen for zinc and carbon steel, which also act as almost perfect absorbents at 65 % RH and above. This effect can be explained by the formation of aqueous adlayers above 60 % RH with properties similar to bulk water on all metals investigated, and the solubility of HNO₃ in water which is at least five orders of magnitude higher than that of SO₂, NO₂, O₃ and H₂S. For the same reason the deposition velocity of HNO₃ is far above that of the other gases.

As a result of nearly perfect absorbing conditions, mass transport of HNO₃ to the metal surface is the rate limiting step in a broad range of exposure conditions. At 65 % RH and 0.03 cm s⁻¹ air velocity, the deposition rate of HNO₃ on copper as well as the corrosion rate turns out to be linearly proportional to HNO₃ concentration up to 400 µg m⁻³. At 65 % RH and 325 µg m⁻³ HNO₃ concentration, the deposition velocity increased with air velocity up to 11.8 cm s⁻¹. In contrast, temperature had no significant effect in the range 15 to 35 °C. It was also shown that the corrosion rate of copper exposed to sub-ppm levels of HNO₃ was nearly constant up to 7 days of exposure and levelled off somewhat after 7 days. This effect may be attributed to weak protective properties of the corrosion products identified under these conditions, cuprite (Cu₂O) and gerhardtite (Cu₂NO₃(OH)₃).

The absolute corrosion rate of carbon steel exposed in HNO₃-containing laboratory air at 65 % RH was approximately three times higher than that of copper or zinc. Compared to the effect of SO₂-containing air, however, the corrosion effect of HNO₃ was the highest for zinc, followed by copper and the lowest for carbon steel.

The nearly perfect absorption of HNO_3 permits the laboratory data, obtained at low air flow rate and high HNO_3 concentration, to be extrapolated to field exposure conditions. A particularly good agreement between laboratory and field data is seen for zinc, where the extrapolated HNO_3 -induced corrosion effect is similar to the HNO_3 effect seen in a dose-response function independently derived from a statistical analysis of field data. Although ambient HNO_3 levels in general are much lower than SO_2 levels, the present study shows that HNO_3 has a significant influence on the atmospheric corrosion of copper and zinc, but not of carbon steel.

With decreasing SO_2 -concentration in many parts of the industrialised world, and unchanged or even increasing HNO_3 concentrations, the results obtained stress the importance of performing similar studies on other materials as well.

5. Future work

Despite the low ambient concentration of HNO_3 this study has shown that even at low concentrations the effects of HNO_3 are of significant relevance for the corrosion of copper and zinc. However, due to the complexity of natural environments it is almost impossible to calculate an accurate corrosion rate of a material in the presence of certain concentration of pollutants. This increases the need for further research and investigations on effects of HNO_3 in the ambient environment, which could lead to new policy making and decreasing concentrations, as has been the case for SO_2 with decreasing SO_2 levels in the last five decades in many countries of the western hemisphere.

A good tool for field studies is exposures of standard materials and climatic and pollutant data acquisitions in order to find connections between corrosion rate and environmental parameters. The field data used in the present study was based on one year exposed metals. At such short exposure time it is almost impossible to evaluate whether the corrosion rate of any material slows down or not. Thus, when the analyses of 2 and 4 years data are available, it will provide a better knowledge on the relation between corrosion rate and important environmental parameters.

The results presented here deal with corrosion of copper, zinc and carbon steel. However, the influence of HNO_3 was also investigated on Portland limestone. The preliminary results show that the deposition velocity of HNO_3 was as high as on a perfect absorbent. Thus, further research on stone materials and other metals are important issues for future work to be performed.

6. Acknowledgements

First of all I would like to thank my supervisors Dr. Johan Tidblad and Prof. Christofer Leygraf. Thank you for believing in me from the start, giving me freedom to develop my research and thank you for your professional skills in supervising. You have taught me a lot! Dr. Vladimir Kucera, with whom I have had the privilege to work with, thanks for your valuable discussions and all conversations about something and everything.

I also want to express my sincere gratitude to the following people (in no specific order) that have, in one way or the other supported me during the time of this doctoral study:

- Dr. Martin Ferm, at the Swedish Environmental Research Institute (IVL), for helpful discussion on HNO₃ measurement and development of the method.
- Dr. Dan Persson, for assistance in FTIR interpretation.
- Dr. Saeid Zakipour, for helpful discussions.
- Mr Lars Göthe, at Stockholm University, for performance of XRD analysis.
- Ms Helen Pahverk, for assistance in field sample preparations and pickling.
- My roommate, Cherry and the entire KIMAB staff for creating such a friendly atmosphere.
- My friend, Mohammed Anan, for all the good times we have had and will have.

I am grateful to my parents, **Jahangir** and **Betty**, for all of your efforts and sacrificing yourselves over and over for us, your children. You left your home, your country, your friends and your family just for us. There is no way I can pay you back, but with these words I want to show that you are appreciated!

My girlfriend, Saideh, thank you for all love, understanding and laughs.

Finally, Farshad, Farshid and Farzad you are my brothers and my best friends too. This thesis is dedicated to you!

فرید سمیعی

Farid Samie

December 2006, Stockholm, Sweden

7. References

- 1 Vernon, W.H.J., 1927. Second experimental report to the atmospheric corrosion research committee (British Non – Ferrous Metals Research Association). *The Faraday Society*, 23, 113-204.
- 2 Cramer, S.D., Covino Jr., B.S., Holcomb, G.R., 1996. Cubic Model for Describing the Atmospheric Corrosion of Structural Metals. 13th International Corrosion Congress, paper 032.
- 3 Cramer, S.D., Matthes, S.A., Covino, B.S. Jr., Bullard, S.J., Holcomb, G.R., 2002. Environmental factors affecting the atmospheric corrosion of copper. *Outdoor Atmospheric Corrosion*, ASTM STP 1421, Townsend, H. E., Ed., American Society for Testing and Materials International, West Conshohocken, PA, 245-264.
- 4 Eriksson, P., Johansson, L.G., 1986. The role of NO₂ in the atmospheric corrosion of different metals. *Proceeding of 10th Scandinavian Corrosion Congress*. 43, Stockholm.
- 5 Golubyev, A.I., Kadyrov, M.Kh., 1968. Metal corrosion forecast under atmospheric conditions. *Corrosion week*, Budapest, 1039-1044.
- 6 Graedel, T.E., 1989. Corrosion mechanisms for zinc exposed to the atmosphere. *Journal of the Electrochemical Society* 136 (4), 193C-203C.
- 7 Graedel, T.E., 1992. Corrosion mechanism for silver exposed to the atmosphere. *Journal of the Electrochemical Society* 139, 1963.
- 8 Graedel, T.E., Frankenthal, R.P., 1990. Corrosion mechanism for iron and low alloy steels exposed to the atmosphere. *Journal of the Electrochemical Society* 137 (8), 2385-2394.
- 9 Graedel, T.E., Nassau, K., Franey, J.P., 1987. Copper patinas formed in the atmosphere – I. Introduction. *Corrosion Science* 27 (7), 639-657.
- 10 Johansson, L.-G., 1984. The corrosion of steel in atmospheres containing small amounts of SO₂ and NO₂. *Proc. 9th Int. Corrosion Congress*, Vol. 1, 407-411.
- 11 Kucera, V., Tidblad, J., Kreislova, K., Knotkova, D., Faller, M., Reiss, D., Snethlage, R., Yates, T., Henriksen, J., Schreiner, M., Melcher, M., Ferm, M., Lefe`vre, R.-A., Kobus, J., 2006. The UN/ECE ICP materials multipollutant exposure on effects on materials including historic and cultural monuments. *Water, Air and Soil Pollution*, accepted for publication.
- 12 Leygraf, C., Graedel, T., 2000. *Atmospheric Corrosion*. Wiley, The Electrochemical Society, INC. Pennington, New York.
- 13 Lipfert, F.W., 1989. Dry deposition velocity as an indicator for SO₂ damage to materials. *Journal of Air Pollution Control Association* 39 (4), 446-452.
- 14 Lipfert, F.W., Benarie, M., Daum, M.L., 1986. Metallic corrosion damage functions for use in environmental assessments. *Proceedings - Journal of the Electrochemical Society*, 86-6, 108-154.

- 15 Phipps, P.B.P., Rice, W., 1979. The role of water in atmospheric corrosion. *American Chemical Society American Chemical Society* 8, 236-261.
- 16 Rice, D., W., Cappell, R., J., Kinsolving, W., Laskowski, J., J., 1980. Indoor corrosion of metals. *Journal of the Electrochemical Society* 127 (4), 891-901.
- 17 Strandberg, H., 1997. Perspectives of bronze sculpture conservation; modelling copper and bronze corrosion. Ph.D. Thesis (ISBN 91-7197-539-X).
- 18 Strekalov, P.V., Agafonov, V.V., Mikhailovski Yu.N., 1972. Effect of temperature on the adsorption of moisture and the corrosion rate of zinc under atmospheric condition. *Protection of Metals* 8, 521-523.
- 19 Strekalov, P.V., Wo, W.D., Mikhailovskii, Y.N., 1983. Kinetics of atmospheric corrosion of steel and zinc in a tropical climate: results of five-year tests. *Protection of Metals* 19 (2), 220-231.
- 20 Svensson, J-E., 1995. The influence of different air pollutants on the atmospheric corrosion of zinc. Ph.D. Thesis (ISBN 91-7197-086-X).
- 21 Tidblad, J., 1994. Atmospheric corrosion of Ni, Cu, Ag and Sn by acidifying pollutants in sheltered environments. – A combined statistical and surface analysis. Ph.D. Thesis (ISBN 91-7170-867-7).
- 22 Tidblad, J., Kucera V., Samie, F., Das, S.N., Bhamornsut, C., Peng, L.C., So, K.L., Dawei, Z., Lien, L.T.H., Schollenberger, H., Lungu, C.V., Simbi, D., 2006. Corrosion impacts of air pollution in developing countries. *Water, Air and Soil Pollution*, accepted for publication.
- 23 Tidblad, J., Kucera, V., Mikhailov, A.A., Henriksen, J., Kreislova, K., Yates, T., Stöckle, B., Schreiner, M., (2001). UN ECE ICP materials: Dose-response functions on dry and wet acid deposition effects after 8 years of exposure. *Water, Air, & Soil Pollution* 130, 1457-1462.
- 24 Tidblad, J., Leygraf, C., 1995. Atmospheric corrosion effects of SO₂ and NO₂: a comparison of laboratory and field exposed copper. *Journal of the Electrochemical Society* 142 (3), 749-756.
- 25 Tidblad, J., Leygraf, C., Kucera, 1993. Acid deposition effects on materials: evaluation of nickel after 4 years of exposure. *Journal of the Electrochemical Society* 140, 1912-1916.
- 26 Volpe, L., Peterson, P., J., 1991. Mass-transport limitations in atmospheric corrosion. Proc. 1st Int. Symp. Corrosion of Electronic Materials and Devices, Seattle, 2, 22-31.
- 27 Leygraf, C., 2002. Atmospheric Corrosion. *Corrosion Mechanism in Theory and Practice* 2nd Edition, edited by Philippe Marcus, 529-562.
- 28 Ferm, M., Watt, J., O'Hanlon, S., De Santis, F., Varotsos, C., 2006. Deposition measurement of particulate matter in connection with corrosion studies. *Analytical and Bioanalytical Chemistry* 384, 1320-1330.
- 29 Eleftheriadis, K., Balis, D., Ziomas, I.C., Colbeck, I., Manalis, N., 1998. Atmospheric Aerosol and Gaseous Species in Athens, Greece. *Atmospheric Environment* 32, 2183-2191.

- 30 Erduran, M.S., Tuncel, S.G., 2001. Gaseous and particulate air pollutants in the Notheastern air pollutants in the Notheastern Mediterranean Coast. *The Science of Total Environment* 281, 205-215.
- 31 Fox, D.L., Stockburger, L., Weathers, W., Spicer, C.W., Mackay, G.I., Schiff, H.I., Eatough, D.J., Mortensen, F., Hansen, L.D., Shepson, P.B., Kleindienst, T.E., Edney, E.O., 1988. Intercomparison of Nitric Acid diffusion denuder methods with tunable diode laser absorption spectrometry. *Atmospheric Environment* 22 (3), 575-585.
- 32 Piringer, M., Ober, E., Puxbaum, H., Hromp-Kolb, H., 1997. Occurrence of Nitric Acid and related Compounds in The Northern Vienna Basin during Summertime Anticyclonic Conditions. *Atmospheric Environment* 31, 1049-1057.
- 33 Tanner, R.L., Valente, R.J., Meagher, J.F., 1998. Measuring inorganic nitrate species with short time resolution from an aircraft platform by dual-channel ozone chemiluminescence. *Journal of Geophysical Research* 103, 22387-22395.
- 34 Ferm, M., De Santis, F., Varotsos, C., 2005. Nitric acid measurements in connection with corrosion studies. *Atmospheric Environment* 39, 6664-6672.
- 35 Pantani, M., Sabbioni, C., Bruzzi, L. and Manco, D., 1998. Air pollution deposition on stones of artistic interest. In *Proc. Air Pollution* 98, 675-684.
- 36 Derwent, R.G., Hertel, O., 1998. Transformation of air pollutants, in: Fenger et al. (Eds.), *Urban Air Pollution – European Aspects*, Kluwer Academic Publishers, Dordrecht, 137-160.
- 37 Pandis, S.N., Seinfeld, J.H., 1989. Sensitivity analysis of a chemical mechanism for aqueous-phase atmospheric chemistry. *Journal of Geophysical Research* 94 (D1), 1105-1126.
- 38 Judd, C.D., Husain, L., 2000. Determination of gas-phase nitric acid using a tracer technique. *Atmospheric Environment* 34, 2333-2341.
- 39 Matsumoto, K., Tanaka, H., 1996. Formation and dissociation of atmospheric particulate nitrate and chloride: an approach based of phase equilibrium. *Atmospheric Environment* 30 (4), 639-648.
- 40 Spicer, C.W., Howes, J.E., Bishop, T.A., Arnold, L.H., Stevens, R.K., 1982. Nitric acid measurements methods: an Intercomparison. *Atmospheric Environment* 16, 1487-1500.
- 41 Fenter, F.F., Caloz, F., Rossi, M.J., 1995. Experimental evidence for the efficient “dry deposition” of nitric acid on calcite. *Atmospheric Environment* 29 (22), 3365-3372.
- 42 Haneef, S.J., Johnson, J.B., Dickinson, C., Thompson, G.E., Wood, G.C., 1992. Effect of dry deposition of NO_x and SO₂ gaseous pollutants on the degradation of calcareous building stones. *Atmospheric Environment* 26A (16), 2963-2974.
- 43 Kirkitsos, P., Sikiotis, D., 1995. Deterioration of Pentelic marble, Portland limestone and Baumberger sandstone in laboratory exposures to gaseous nitric acid. *Atmospheric Environment* 29 (1), 77-88.
- 44 Sikiotis, D., Kirkitsos, P., 1995. The adverse effects of nitrates on stone monuments. *The Science of Total Environment* 171, 173-182.

- 45 Lipfert, F.W., 1989. Atmospheric damage to calcareous stones: comparison and reconciliation of recent experimental findings. *Atmospheric Environment* 23 (2), 415-429.
- 46 Cramer, S.D., Covino Jr., B.S., Holcomb, G.R., 1996. Cubic Model for Describing the Atmospheric Corrosion of Structural Metals. 13th International Corrosion Congress, paper 032.
- 47 Tidblad, J., Kucera, K., Samie, F., Schreiner, M., Melcher, M., Kreislova, K., Knotkova, D., Lefèvre, R.-A., Ionescu, A., Snethlage, R., Varotsos, C., De Santis, F., Mezinskis, G., Sidraba, I., Henriksen, J., Kobus, J., Ferm, M., Faller, M., Reiss, D., Yates, T., Watt, J., Hamilton, R., O'Hanlon, S., 2004. Publishable final report of the EU 5FP RTD Project "Model for multi-pollutant impact and assessment of threshold levels for cultural heritage" (MULTI-ASSESS). Contract number: EVK4-CT-2001-00044.
- 48 Ferm, M., 2002. Personal communication, email: martin.ferm@ivl.se
- 49 Ferm, M., 2001. Validation of diffusive sampler for ozone in workplace atmospheres according to EN 838. *Proceedings International Conference Measuring Air Pollutants by Diffusive Sampling*, 298-303.
- 50 Allegrini, I., De Santis, F., Di Palo, V., Febo, A., Perrino, C., Possanzini, M., 1987. Annular Denuder for Sampling Reactive Gases and Aerosols in the Atmosphere. *The Science of the Total Environment*, 67, 1-16.
- 51 Ferm, M., Sjödin, Å., 1985. A sodium carbonate coated denuder for determination of nitrous acid in the atmosphere. *Atmospheric Environment* 19 (6), 979-983.
- 52 Ferm, M., 1986. A Na₂CO₃-coated denuder and filter for determination of gaseous HNO₃ and particulate NO₃⁻ in the atmosphere. *Atmospheric Environment* 20 (6), 1193-1201.
- 53 Bollinger, M.J., Sievers, R.E., Fahey, D.W., Fehsenfeld, F.C., 1983. Conversion of nitrogen dioxide, nitric acid and n-propyl nitrate to nitric oxide by gold-catalyzed reduction with carbon monoxide. *Analytical Chemistry* 55, 1980-1986.
- 54 Neuman, J.A., Huey, L.G., Ryerson, T.B., Fahey, D.W., 1999. Study of inlet materials for sampling atmospheric nitric acid. *Environmental Science and Technology* 33, 1133-1136.
- 55 Tidblad, J., Leygraf, C., 1995. Atmospheric corrosion effects of SO₂ and NO₂: a comparison of laboratory and field exposed copper. *Journal of the Electrochemical Society* 142 (3), 749-756.
- 56 Lipfert, F.W., Wyzga, R.E., 1986. Application of a theory for economic assessment of corrosion damage. *American Chemical Society (Symposium Series)*, 411-430.
- 57 Smith, R.I., Fowler, D., Sutton, M.A., Flechard, C., Cole, M., 2000. Regional estimation of pollutant gas dry deposition in the UK: Model Description, Sensitivity Analyses and Outputs. *Atmospheric Environment* 34, 3757-3777.
- 58 Graedel, T.E., Nassau, K., Franey, J.P., 1987. Copper patinas formed in the atmosphere – I. Introduction. *Corrosion Science* 27 (7), 639-657.
- 59 Scott, D.A., 2002. Copper and bronze in art. Corrosion, colorants, conservation. The Getty Conservation Institute Los Angeles. Ch.7 Copper Phosphates and Copper Nitrates, 240-251.

- 60 Volpe, L., Peterson, P., J., 1989. The atmospheric sulfidation of silver in a tubular corrosion reactor. *Corrosion Science* 29, 1179-1196.
- 61 Volpe, L., Peterson, P., J., 1993. Indoor gaseous sulfide and chloride pollutants and their reaction with silver. Proc. 12th Int. Corrosion Congress, Houston, 590-599.
- 62 Durham, J.L., Stockburger, L., 1986. Nitric acid-air diffusion coefficient: Experimental determination. *Atmospheric Environment* 20 (3), 559-563.
- 63 Benner, C.L., Eatough, N.L., Lewis, E.A., Eatough, D.J., Huang, A.A., Ellis, E.C., 1988. Diffusion coefficients for ambient nitric and nitrous acids from denuder experiments in the 1985 nitrogen species methods comparison study. *Atmospheric Environment* 22 (8), 1669-1672.
- 64 Dollard, G.J., Atkins, D.H.F., Davies, T.J., Healy, C., 1987. Concentrations and dry deposition velocities of nitric acid. *Nature* 326, 481-483.
- 65 Hanson, P.J., Lindberg, S.E., 1991. Dry deposition of reactive nitrogen compounds: a review of leaf, canopy and non-foliar measurements. *Atmospheric Environment* 25A (8), 1615-1634.
- 66 Rodhe, H., 1991. Luftföroreningars Spridning. (In Swedish), Compendium, University of Stockholm, Sweden.
- 67 Sievering, H., Rusch, D., Marquez, L., 1996. Nitric acid, particulate nitrate and ammonium in the continental free troposphere: nitrogen deposition to an alpine tundra ecosystem. *Atmospheric Environment* 30 (14), 2527-2537.
- 68 Barton, K., 1973. Schutz gegen atmosphärische Korrosion, Theorie und Technik. Verlag Chemie GMBH Weinheim, Germany. (*In German*)
- 69 Golubyevev, A.I., Kadyrov, M.Kh., 1968. Metal corrosion forecast under atmospheric conditions. *Corrosion week*, Budapest, 1039-1044.
- 70 Oesch, S., Faller, M., 1997. Environmental effects on materials: the effect of the air pollutants SO₂, NO₂, NO and O₃ on the corrosion of copper, zinc and aluminium. A short literature survey and results of laboratory exposures. *Corrosion Science* 39 (9), 1505-1530.
- 71 Strandberg, H., Johansson, L.G., 1997. Role of O₃ in the atmospheric corrosion of copper in the presence of SO₂. *Journal of the Electrochemical Society* 144 (7), 2334-2342.
- 72 Bjerrum, J., 1931 (In German). Untersuchungen Über Kupferammoniakverbindungen I. Bestimmung der Komplexitätskonstanten der Amminkupriionen Durch Ammoniak tensionsmessungen und durch Löslichkeitsbestimmungen mit Basischem Kuprinitrat (Gerhardtit). *Mathematisk-fysiske Meddelelser XI*, 5. Det Kgl. Danske Videnskabernes Selskab.
- 73 Graedel, T.E., 1987. Copper patinas formed in the atmosphere – III. A semi-quantitative active assessment of rates and constraints in the greater New York metropolitan area. *Corrosion Science* 27 (7), 741-769.
- 74 New, M., Lister, D., Hulme, M., Makin, I., 2002. A high-resolution data set of surface climate over global land areas. *Climate Research* 21, 1-25.